

# Efficient temporal shaping of ultrashort pulses with birefringent crystals

Shian Zhou,<sup>1,\*</sup> Dimitre Ouzounov,<sup>2</sup> Heng Li,<sup>1</sup> Ivan Bazarov,<sup>2</sup> Bruce Dunham,<sup>2</sup> Charles Sinclair,<sup>2</sup> and Frank W. Wise<sup>1</sup>

<sup>1</sup>Department of Applied and Engineering Physics, Cornell University, Ithaca, New York 14853, USA

<sup>2</sup>Physics Department, LEPP and CHESS, Cornell University, Ithaca, New York 14853, USA

\*Corresponding author: sz53@cornell.edu

Received 18 May 2007; revised 3 October 2007; accepted 12 October 2007;  
posted 15 October 2007 (Doc. ID 83158); published 7 December 2007

We report on a simple and robust technique to temporally shape ultrashort pulses. A number of birefringent crystals with appropriate crystal length and orientation form a crystal set. When a short pulse propagates through the crystal set, the pulse is divided into numerous pulses, producing a desired temporal shape. Flexibility in the final pulse shape is achieved through varying initial pulse duration, divided-pulse number, the polarization-mode delay, and energy distribution of the divided pulses. The energy efficiency of the technique is near 100% for a pulse train of alternating polarizations, and 50% for a linearly polarized pulse train. © 2007 Optical Society of America

*OCIS codes:* 320.5540, 320.7080.

## 1. Introduction

Shaping of ultrashort laser pulses is an area of active research. Potential applications include coherent control of chemical reactions, pulse train generation for telecommunications, generation of large-amplitude plasma waves [1], driving photo-emission electron sources for various accelerator physics applications [2,3], multiple-pulse excitation of atoms, molecules, and solids [4], and generation of terahertz radiation [5].

Pulses can be shaped directly in the time domain by the use of a modulator. However, there are no electronic devices that can operate on the picosecond or femtosecond time scales. Pulse-shaping techniques in the spectral domain have been developed to shape ultrafast pulses. Using one of these techniques, the spectral content of the incoming pulse is dispersed in space, and each frequency component is mapped to a unique position on a plane. By placing a mask or a spatial light modulator (SLM) (liquid crystal [6], acousto-optical [7], or deformable mirrors [8] in the plane, either the phase or amplitude of each spectral

component can be controlled or modified. This powerful approach, in principle, offers full control of the pulse spectrum and provides the capability for generating arbitrary shapes. The experimental setup is relatively complicated, and misalignments can produce spatiotemporal distortions of the field. Another method based on acousto-optic interaction in birefringent crystal has been proposed [9] and demonstrated. The input pulse is polarized along the ordinary axis and interacts with a polychromatic acoustic wave. At different positions along the direction of propagation, different frequency components satisfy phase-matching conditions and their polarization is rotated toward the extraordinary axis. The setup is simpler than that based on the SLM, and it does not introduce spatiotemporal distortion. However, this method is inapplicable for high repetition rate ( $>100$  kHz) pulse trains, which are encountered in many applications. Previous works [10, 11] demonstrated dividing a pulse into two or four pulses in one or two birefringent crystals, where the pulse shaping was controlled by a polarizer. An  $n$ -stage Michelson interferometer was proposed to generate  $2^n$  pulses with high efficiency [12].

Here, we report on a new approach to temporally shape ultrashort pulses. Building on the work of

[10] and [11], we employ a sequence of birefringent crystals to produce an ultrashort pulse train. We extend our previous results from [13]. The pulse train structure is similar to that of [12], but here we apply birefringent crystals instead of the Michelson interferometer. The pulse train with alternating polarizations can form pulse bursts, for example a super-Gaussian (flat-top) shape. For applications insensitive to pulse polarizations, the pulse shaping is nearly lossless; the shaping efficiency can be 50% for applications that require linear polarization. This method is compatible with femtosecond or picosecond pulses, high or low repetition rate, and high or low peak power.

## 2. Shaper Design

The main principle of this method is to implement a birefringent crystal sequence to divide a pulse into several smaller pulses with equal pulse durations, and recombine these pulses with temporal offsets and varying amplitudes to form a target shape. The final shape can be tailored for a particular application by varying the parameters of the crystals.

We begin by briefly reviewing the properties of birefringent crystals. A wave is defined as ordinary (*o*-wave) if the polarization of the incident light lies in the plane of incidence, or as extraordinary (*e*-wave) if it is perpendicular to the plane. The laser pulse can be divided into two pulses as long as its polarization is not along the optical axis (OA) of the crystal. In general, the *o*- and *e*-waves will have distinct group velocities.

Various pulse shapes can be obtained by changing the number of subpulses, the polarization-mode delay, the energy distribution among the divided pulses, and the initial pulse duration. With  $n$  crystals, the pulse shaper generates  $2^n$  divided pulses (Fig. 1). For simplicity, we set the angle between the incident (linear) laser polarization and the OA of the first crystal to  $45^\circ$ , which divides a pulse into two with equal intensities. Other angles will produce different shapes. The OA of the second crystal has the same orientation as the polarization of the incident pulses. The OA of the third crystal is in the same orientation as that of the first crystal. As a consequence, the OA orientations of the birefringent crystals at all odd-numbered positions are the same, at a  $45^\circ$  angle to the laser polarization; and all of those at the even-numbered positions are pointed in the same

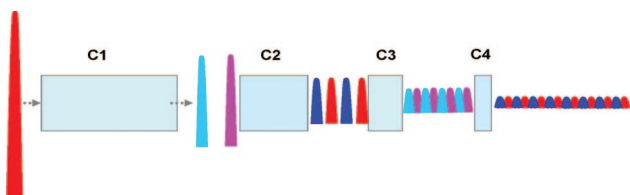


Fig. 1. (Color online) Principle of pulse shaping. C1–C4 are *a*-cut YVO<sub>4</sub> crystals. Each shade (color) of the pulses presents one orientation of polarization. The output pulse sequence has alternating linear polarizations.

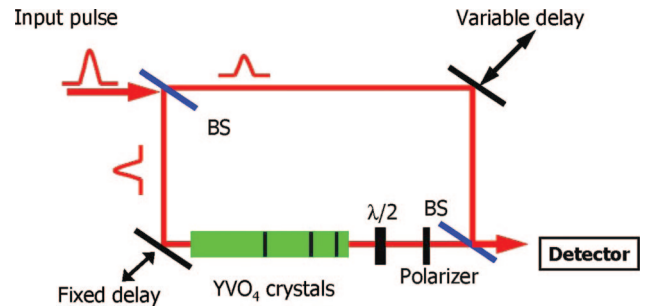


Fig. 2. (Color online) Schematic of the cross correlator. BS, beam splitter.

direction and are parallel to the polarization of the incident light, (Fig. 1). We employed the *a*-cut YVO<sub>4</sub> in experiments because it has relatively large group delay between polarizations. Other birefringent crystals should lead to similar results. The insertion loss of each crystal with antireflection coating is less than 0.2%, so that the total loss of the crystal stack can be made negligible.

The pulse spacing is adjustable by varying the corresponding crystal length. For the sake of simplicity, we use equal separation,  $t = l_0(1/v_e - 1/v_o)$ , between all neighboring pulses. Here,  $v_o$  and  $v_e$  are the group velocities of the *o*- and *e*-waves, respectively, and we assume that  $v_o > v_e$ . If the first crystal length is  $l_0$ , the length of the  $m$ th crystal should be  $l_m = 2^{m-1}l_0$  to achieve equal pulse spacing. After the pulses pass the crystal stack, the resulting pulse is composed of  $2^m$  equidistant pulses of the same width. The  $i$ th pulse from the pulse front is delayed by  $T_i = (2^m - 1)l_0/v_o + (i - 1)l_0(1/v_e - 1/v_o)$ .

When the number of crystals is even, the odd-numbered pulses in the sequence have the same polarization as the incident pulse; the even-numbered pulses have the perpendicular polarization. If the number of crystals is odd, the odd-numbered pulses have the same polarization as the OA of the first crystal; the polarization of the even-numbered pulses is perpendicular to that of odd-numbered pulses. The orthogonally polarized pulses interleave. Pulse division in a crystal stack is schematically shown in Fig. 1. Long crystals can be created by abutting two short crystals with the same orientation of the OA and surface.

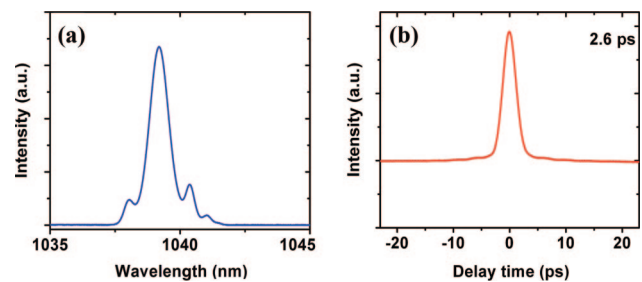


Fig. 3. (Color online) (a) Source spectrum, (b) autocorrelation of source pulse.

### 3. Experiments and Results

Our particular interest is finding a simple and robust means for shaping picosecond-duration pulses that will drive a high-brightness electron source [2], but this method could be extended to femtosecond pulse-shaping. A cross correlator shown in Fig. 2 is implemented to measure the pulse shape after the crystal stack. A half-wave plate and a polarizer select the polarization of the shaped pulse. The half-wave plate rotates the pulse polarization to the same orientation as that of the sampling pulse. The polarizer is set at a  $45^\circ$  angle to both polarizations of the shaped pulses.

We demonstrate some examples of pulse shapes by changing the crystal lengths in a crystal stack. We

use five different length crystals for simulation and experiment: 4.2, 8, 10, 15.4, and 22 mm. The spectrum of the seed pulse is presented in Figure 3(a) (center wavelength is 1038 nm and the bandwidth is approximately 0.8 nm), and the pulse duration is approximately 2.6 ps [Fig. 3(b)]. First, the cross correlations of the pulse-shaped, pulse burst, or variable pulse duration, by the combination of 15.4 and 8 mm crystals, is shown in Fig. 4(b), by 8 and 4.2 mm crystals in Fig. 4(d), and by 22 and 10 mm crystals in Fig. 4(f). Figures on the left side of Fig. 4 are the corresponding pulse shapes obtained through simulation with the same parameters as the right side. The shaped pulses are measured by cross correlation with

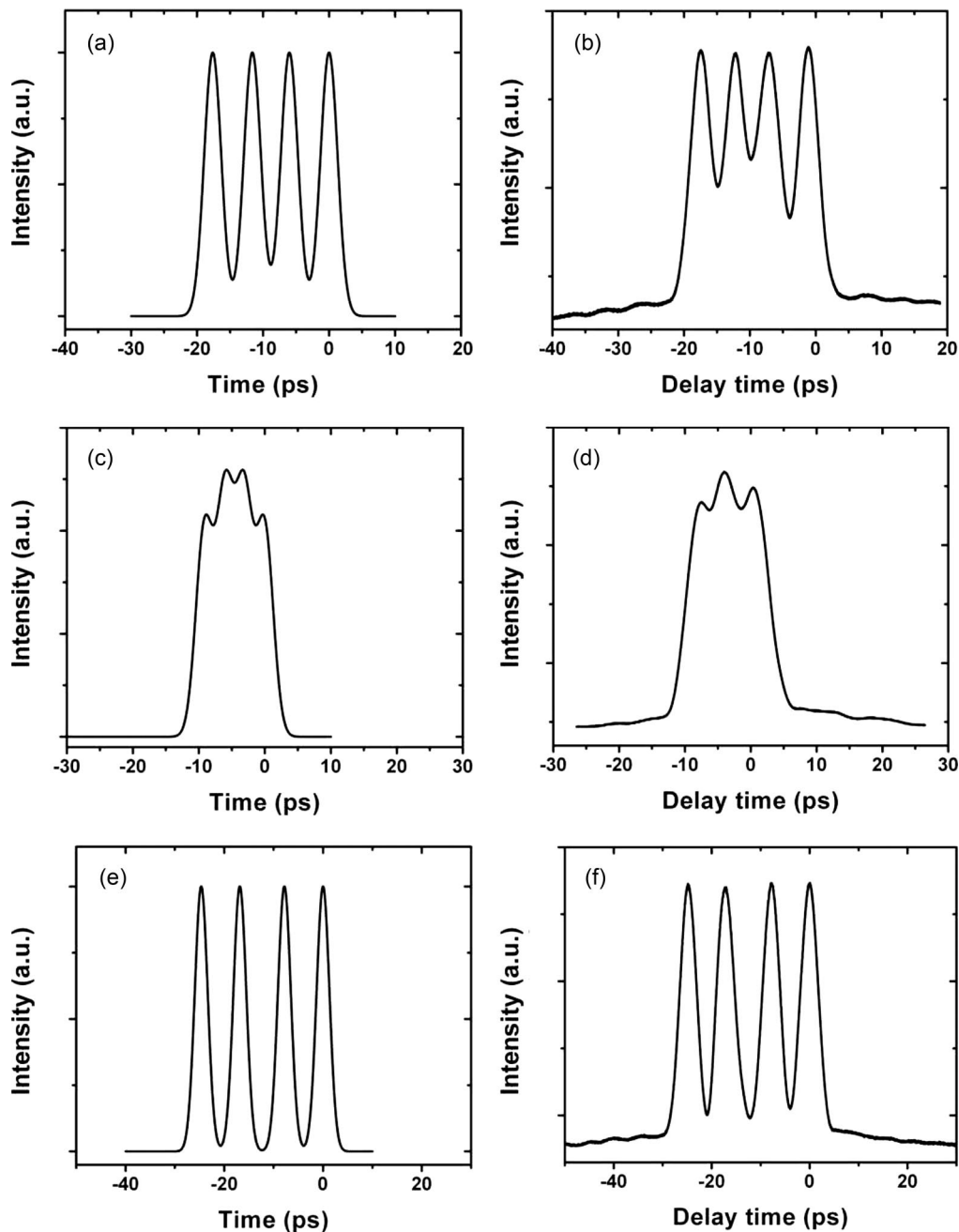


Fig. 4. Pulse shaping by crystal stacking. Left side, simulations. Right side, corresponding experimental results.

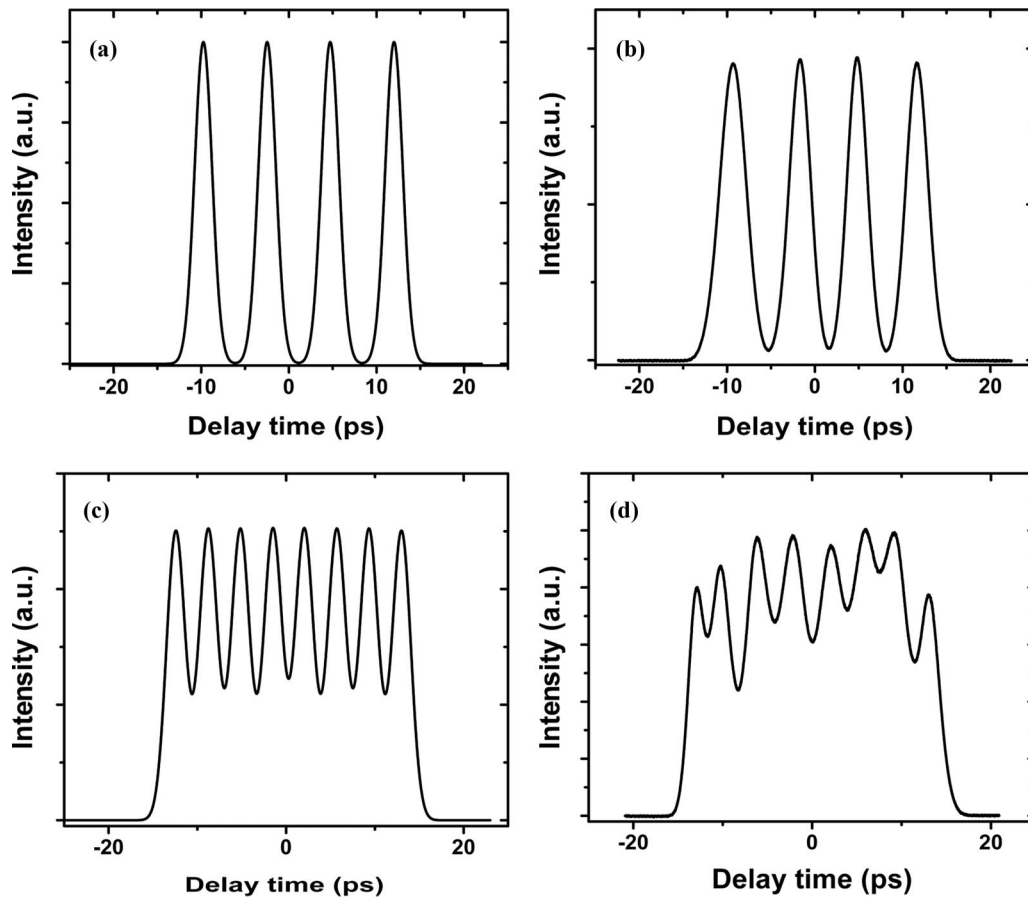


Fig. 5. Pulse shaping at 520 nm. (a) Simulated pulse burst produced with 6.9 and 13.7 mm  $\text{YVO}_4$  crystals; (b) experimental results corresponding to (a); (c) simulated pulse burst produced with 3.5, 6.9, and 13.7 mm  $\text{YVO}_4$  crystals; (d) experimental results corresponding to (c).

the 2.6 ps pulse sampling pulse. Second, a 2 ps seed pulse at 519 nm wavelength is launched to demonstrate the pulse shaping at a different wavelength in Fig. 5. Further, a series of experiments was performed to confirm the interleaved construction of the shaped pulses by rotating the half-wave plate. Since the sampling pulse duration is more than 2 ps, the temporal resolution of the cross correlations is limited to this value. We also verify the interleaved structure of the pulse polarization by rotating the half-wave plate and measuring the cross correlation. Although the low resolution limits some minor information, overall the measured shapes agree well with the numerical results. The results of Fig. 5(d) illustrate a property of the pulse-shaping technique when the subpulses overlap significantly in time: Interference between polarization components generated in separate crystals produces a dependence on the path lengths through the crystals on the scale of the wavelength. In practice, the actual shape is quite sensitive to the orientation of the crystals through inadvertent tilts. The discrepancy between the measured pulse [Fig. 5(d)] and the target pulse [Fig. 5(c)] is typical.

Extensions to more crystals and the generation of more divided pulses are straightforward. For instance, simulation results of pulse shaping by five-

crystal stacks are shown in Fig. 6. First, we use a 200 fs pulse to generate a 32-pulse burst by a five-crystal stack [Fig. 6(a)]. The last crystal length is approximately 1.06 mm, and the pulse spacing is approximately 800 fs. The pulse burst is desirable for telecommunication. The generation of square or flat-topped pulses is complicated by the interference effect discussed in connection with Fig. 6(d). If the time interval between 200 fs subpulses is reduced to 150 fs by use of another five-crystal stack ending with a 0.2 mm crystal, the generated pulse is square overall but exhibits  $\sim 15\%$  modulation owing to interference.

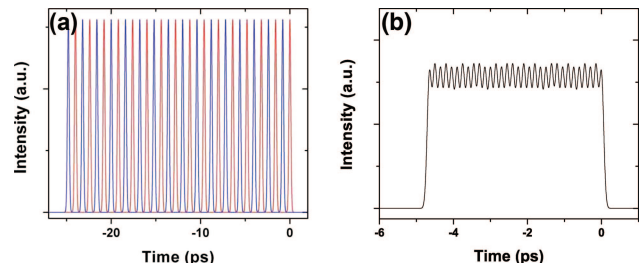


Fig. 6. (Color online) Simulation results of pulse shaping by five-crystal stack: (a) burst of 32 200 fs pulses with large spacing, (b) square pulse produced by 32 200 fs pulses with small spacing.



Pulse shaping by birefringent crystals offers such promising properties as low insertion loss, applicability to both femtosecond and picosecond pulse-duration ranges, and large transparency range. Implementation of this pulse shaping with  $\sim 100$  fs pulses will require control of the crystal lengths to  $\sim 10$   $\mu\text{m}$ , which is readily achievable. Some form of dispersion control will also be needed. A simple approach might be to choose birefringent materials with small group-velocity dispersion. However, the difference in the dispersions for *o*- and *e*-waves will ultimately limit the control over the shaped pulse. In general, the created optical field will be a superposition of the orthogonal polarizations projected by the crystals. For applications that require linearly polarized light, a polarizer is placed after the series of crystals. The pulse shape will then be influenced by interference between adjacent subpulses in situations where they overlap temporally. This complicates the direct measurement of the pulse shape, and will also limit the accuracy of the pulse shaping. After the submission of this manuscript, research was published that reported the generation of a train of  $\sim 40$  fs pulses by the same technique described here, but used calcite crystals, not birefringent ones [14]. This demonstrates the extension of birefringent pulse shaping to the sub-100 fs regime.

#### 4. Conclusion

We propose and demonstrate a simple new approach to shape ultrashort pulses, based on birefringent crystals. This method extends the principle of the previous work leading to the great flexibility of achievable pulse shapes. It also offers a number of advantages: low insertion loss, simplicity, robustness, large working bandwidth, and compatibility with a wide range of repetition rates. The shaped pulse satisfies many practical requirements, especially in terms of pulse burst and pulse amplification with low nonlinear distortion, and, in particular, it is well suited for the photocathode injector under development at Cornell University.

This work was supported by the National Science Foundation under grants ECS-0500956 and PHY-0131508, and by the Laboratory for Elementary Particle Physics and Cornell High Energy Synchrotron

Source at Cornell University. S. Zhou acknowledges inspiring discussions with W. Condit.

#### References

1. D. Umstadter, E. Esarey, and J. Kim, "Nonlinear plasma waves resonantly driven by optimized laser pulse trains," *Phys. Rev. Lett.* **72**, 1224–1227 (1994).
2. H. Tomizawa, T. Asaka, H. Dewa, H. Hanaki, T. Kobayashi, A. Mizuno, S. Suzuki, T. Taniuchi, and K. Yanagida, "Development of adaptive feedback control system of both spatial and temporal beam shaping for UV-laser light source for RF gun," in *Proceedings of LINAC 2004* (2004), pp. 207–209.
3. I. V. Bazarov and C. K. Sinclair, "Multivariate optimization of a high brightness dc gun photoinjector," *Phys. Rev. ST Accel. Beams* **8**, 034202 (2005).
4. R. J. Temkin, "Excitation of an atom by a train of short pulses," *J. Opt. Soc. Am. B* **10**, 830–839 (1993).
5. J. Ahn, A. Efimov, R. Averitt, and A. Taylor, "Terahertz waveform synthesis via optical rectification of shaped ultrafast laser pulses," *Opt. Express* **11**, 2486–2496 (2003).
6. A. M. Weiner, D. E. Leaird, J. S. Patel, and J. R. Wullert II, "Programmable shaping of femtosecond optical pulses by use of 128-element liquid crystal phase modulator," *IEEE J. Quantum Electron.* **28**, 908–920 (1992).
7. M. A. Dugan, J. X. Tull, and W. S. Warren, "High-resolution acousto-optic shaping of unamplified and amplified femtosecond laser pulses," *J. Opt. Soc. Am. B* **14**, 2348–2358 (1997).
8. E. Zeek, K. Maginnis, S. Backus, U. Russek, M. Murnane, G. Mourou, and H. Kapteyn, "Pulse compression by use of deformable mirrors," *Opt. Lett.* **24**, 493–495 (1999).
9. F. Verluise, V. Laude, Z. Cheng, C. Spielmann, and P. Tournais, "Amplitude and phase control of ultrashort pulses by use of an acousto-optic programmable dispersive filter: pulse compression and shaping," *Opt. Lett.* **25**, 575–577 (2000).
10. H. E. Bates, R. R. Alfano, and N. Schiller, "Picosecond pulse stacking in calcite," *Appl. Opt.* **18**, 947–949 (1979).
11. C. Radzewicz, M. J. La Grone, and J. S. Krasinski, "Passive pulse shaping of femtosecond pulses using birefringent dispersive media," *Appl. Phys. Lett.* **69**, 272–274 (1996).
12. C. W. Siders, J. L. W. Siders, A. J. Taylor, S. Park, and A. M. Weiner, "Efficient high-energy pulse-train generation using a 2<sup>nd</sup>-pulse Michelson interferometer," *Appl. Opt.* **37**, 5302–5305 (1998).
13. S. Zhou, D. G. Ouzounov, F. W. Wise, I. Bazarov, and C. Sinclair, "Efficient temporal ultrashort pulse shaping with birefringent crystals," *Conference on Lasers and Electro-Optics* (Optical Society of America, 2007), paper CTuFF3.
14. B. Dromey, M. Zepf, M. Landreman, K. O'Keeffe, T. Robinson, and S. M. Hooker, "Generation of a train of ultrashort pulses from a compact birefringent crystal array," *Appl. Opt.* **46**, 5142–5146 (2007).